Acta Chemica Scandinavica, 1999: 53: 1013–1022
Printed in UK. All rights reserved

ACTA
CHEMICA SCANDINAVICA
ISSN 0904–213X

Mechanism of the Dissociative Electro-oxidation of Oxalate in Aprotic Solvents

Abdirisak A. Isse, Armando Gennaro* and Flavio Maran*

Dipartimento di Chimica Fisica, Università di Padova, via Loredan 2, 35131 Padova, Italy

Dedicated to Professor Henning Lund on the occasion of his 70th birthday.

Isse, A. A., Gennaro, A. and Maran, F., 1999. Mechanism of the Dissociative Electro-oxidation of Oxalate in Aprotic Solvents. – Acta Chem. Scand. 53: 1013–1022. © Acta Chemica Scandinavica 1999.

The oxidation of oxalate has been studied in dipolar aprotic solvents. The process is characterized by two voltammetric oxidation peaks and proceeds by a dissociative electron transfer mechanism, in which two carbon dioxide molecules are formed with consumption of 2 F mol^{-1}. Voltammetric and convolution analyses of the first peak are in agreement with a stepwise mechanism in which a radical anion forms and then undergoes C–C bond cleavage. By analysis of the potential dependence of the transfer coefficient α, the standard potential was estimated to be 0.06 V vs. SCE in DMF. The carbon dioxide molecules released at the first peak interact with the starting material itself to form an adduct that can be oxidized at the second peak. As a consequence, when the potential is positive enough both the free and the complexed oxalate ions compete in the overall electro-oxidation, as supported by convolution analysis of the heterogeneous electron transfer at the second peak. The voltammetric pattern is quite sensitive to the presence of acids. In the presence of water, in particular, considerable positive shifts of the actual potential for the oxidation of oxalate were observed. This has been related to the formation of a water–oxalate adduct, although the actual species undergoing the electro-oxidation seems to be always the free oxalate ion. The consequences of this effect are discussed.

The electrochemical oxidation of carboxylates, RCO_2^-, has received much attention as a convenient and versatile way of preparing coupling products, R–R. The process is known as the Kolbe electrosynthesis and several reviews are available in the literature.[1–4] This electrode process has been extensively investigated and most mechanistic aspects are now sufficiently clear. Whereas the majority of the studies were carried out in aqueous or alcoholic solutions using Pt electrodes, where substantial modification of the electrode surface is caused by adsorption of reactants and intermediates, the electro-oxidation of carboxylates in dipolar aprotic solvents has been much less investigated. However, basically the same reaction mechanism as in aqueous or alcoholic medium is assumed.[5] It is generally accepted that the Kolbe electrosynthesis of coupling products R_2 follows a free radical sequence initiated by electron transfer from the carboxylate to the electrode, leading to the formation of CO_2 and the radical R$^\cdot$ [eqn. (1) or eqn. (2)], followed by the coupling reaction [eqn. (3)].

$$RCO_2^- - e \rightarrow RCO_2^\cdot \rightarrow R^\cdot + CO_2 \quad (1)$$

$$RCO_2^- - e \rightarrow R^\cdot + CO_2 \quad (2)$$

$$R^\cdot + R^\cdot \rightarrow R\text{–}R \quad (3)$$

It is not clear, however, whether the species undergoing the actual chemical reactions are adsorbed or free radicals in solution.[1–4,5a,c,d,6] Likewise, the mechanism of the oxidative C–C bond cleavage has been matter of discussion.[5c,7,8] In fact, the oxidation could involve the formation of $RCO_2^\cdot$ as a discrete, though labile, intermediate [eqn. (1)], or electron transfer and carbon–carboxyl bond cleavage could be concerted [eqn. (2)]. Indeed, it should be remembered that the dissociative oxidation of carboxylates was considered as the first possible example (together with the dissociative reduction of alkyl halides) of a concerted electron transfer–bond fragmentation reaction.[8,9] Although there are reactions in which oxidative decarboxylations are represented as concerted processes[10] or where irreversible modification of the electrode surface prevents any mechanistic analysis,[5a] clear evidence for the transient formation of the $RCO_2^\cdot$ radicals in homogeneous reactions has sometimes been obtained. In fact, a number of studies based on flash photolysis experiments provided measurable lifetimes for acyloxyl radicals generated either from photodecomposition of dibenzoyl peroxides, peresters, and esters or by

* To whom correspondence should be addressed.

photoinduced electron transfer from carboxylate ion to appropriate acceptors.[11-13] Although the C–C cleavage rate constants so far determined are usually very large (10^9–10^{11} s^{-1}),[12,13] it was found that decarboxylation of aroyloxyl radicals can be relatively slow, the rate constants being of the order of 10^6 s^{-1}.[11] On the basis of the present state of the art we thus conclude that it seems rather unlikely that oxidative decarboxylations proceed according to a concerted dissociative mechanism.

The electro-oxidation of the oxalic acid system is peculiar with respect to that of other mono- or di-carboxylic acids in that it proceeds with formation of two CO_2 molecules in an overall two-electron process. This happens upon oxidation of oxalic acid in aqueous solutions at both Pt and Au electrodes[14] or of oxalate in aprotic solvents (MeCN and Me_2SO).[15] It was reported that the electro-oxidation of $C_2O_4^{2-}$ in MeCN is characterized by a single well-defined irreversible voltammetric peak at Pt and glassy carbon electrodes.[15a,c] The process does not appear to involve adsorbed species. This is an interesting feature if we consider that, e.g., the electro-oxidation of arylacetic acids has been shown to lead to derivatization of carbon surfaces.[5a] In connection with an on-going study on the kinetic and thermodynamic characterization of the relevant intermediates formed in the electrochemical reduction of carbon dioxide in dipolar aprotic solvents, such as oxalate itself,[16] we observed that the voltammetric oxidation of $C_2O_4^{2-}$ at Pt, Au or glassy carbon electrodes gives rise to two irreversible anodic peaks. We found also that the relative heights of the two oxidation peaks are strongly affected by the presence of CO_2, even when present at very low concentrations. These findings prompted us to investigate in detail the mechanism of the anodic oxidation of the oxalate ion in *N,N*-dimethylformamide (DMF) and MeCN. Since we also found no evidence for adsorption of reactant or oxidation intermediates, particular focus was put on unraveling the mechanism of the heterogeneous process, in an attempt to test the Savéant theory of dissociative electron transfer[17] on this type of system. This is an interesting issue because the only clear-cut examples of concerted dissociative electron transfers have been found in the field of reductive processes, in particular the reduction of alkyl halides[18,19] and of peroxides.[20] On the other hand, as previously mentioned, electro-oxidation of carboxylate anions has sometimes been described as a likely example of dissociative electron transfer.[8,9] To date, however, no experimental system has been studied from this point of view by using the necessary theoretical background and the methodologies nowadays available. In this framework, the oxalate anion is a peculiar carboxylate, liable in principle to undergo a concerted dissociative oxidation. In this paper we report the results that we obtained by studying the electro-oxidation of $C_2O_4^{2-}$ in DMF and MeCN, using glassy carbon electrodes. The oxidation was analyzed by using both conventional voltammetric criteria[21] and the convolution approach,[22] a convenient and powerful method to obtain relevant information on heterogeneous dissociative electron transfers.[20c,d,f,23] In addition, we carried out some electro-oxidation experiments in the presence of foreign acidic species, such as carbon dioxide, water, or trifluoroethanol, to obtain complementary information on the investigated process.

Experimental

Chemicals. *N,N*-Dimethylformamide (Janssen, 99%) was purified as previously described.[20c] Acetonitrile was distilled over CaH_2 and stored under an argon atmosphere. The supporting electrolyte was tetraethylammonium perchlorate (Fluka) that had been recrystallized twice from ethanol and dried at 60 °C under vacuum. Tetrabutylammonium oxalate ($[Bu_4N]_2C_2O_4$) was prepared by neutralization of oxalic acid with tetrabutylammonium hydroxide in water, followed by evaporation and drying at 60 °C under vacuum. The resulting white solid is hygroscopic and thus stock solutions in DMF or MeCN were prepared, under a nitrogen atmosphere, from the freshly dried salt. The effective concentration of $[Bu_4N]_2C_2O_4$ in the stock solutions was determined by titration with $KMnO_4$ according to a known procedure.[24] $HC_2O_4^-$ was generated *in situ* by adding an equivalent amount of perchloric acid to a solution of $C_2O_4^{2-}$. CO_2 solutions were prepared by saturating the solvent with appropriate mixtures of CO_2 and argon, as previously described.[25]

Electrochemistry. The glassy carbon (Tokai GC-20) electrode was prepared and activated before each measurement as previously described.[20c] The reference electrode was Ag/AgI/Bu_4NI 0.1 M DMF, calibrated after each experiment against the ferrocene/ferricinium couple; in the presence of 0.1 M Et_4NClO_4, E°_{Fc/Fc^+} is 0.475 and 0.450 V versus the KCl saturated calomel electrode (SCE) in DMF and in MeCN, respectively.[20a] Since the oxidation of ferrocene and that of oxalate partially overlap, calibration was carried out after neutralization of oxalate with perchloric acid. In the following, all of the potential values are reported against SCE. The counterelectrode was a 1 cm^2 Pt plate. Controlled-potential bulk electrolyses were performed in a divided cell using a glassy carbon (Tokai GC-20) rotating cylinder or a platinum grid as the working electrode. Electrochemical measurements were conducted in an all glass cell, thermostatted at 25 °C. The electrochemical instrumentation employed for the electrochemical experiments was EG&G-PARC 173/179 potentiostat-digital coulometer, EG&G-PARC 175 universal programmer, Nicolet 3091 12-bit resolution digital oscilloscope, and Amel 863 X/Y pen recorder. Feedback correction was applied in order to minimize the ohmic drop between the working and reference electrodes. The confidence in the correction was judged as previously described.[20c,d] In most of the experiments, the cyclic voltammograms were recorded in a selected potential range and for scan rates

ranging from 0.1 to 200 V s^{-1} (first in the absence and then in the presence of the carboxylate) by the digital oscilloscope (digitalized 1 point/mV) and then transferred to a PC. The background-subtracted curves were then analyzed by conventional voltammetric criteria[21] or the convolution approach,[20c,22] using our own laboratory software.

Results and discussion

The voltammetric oxidation of $C_2O_4^{2-}$ gives rise to two irreversible oxidation peaks in either DMF or MeCN. Typical peak potential (E_p) values measured at the first peak for different scan rate (v) values are reported in Table 1, together with other electrochemical data. The electrode material of choice was glassy carbon. On this electrode material, no complications due to surface interaction of the substrate and/or of its oxidation intermediates were apparent in the voltammetric behavior. In fact, the voltammetric pattern was reproducible over a prolonged period of time and no passivation of the electrode was observed upon repetitive cycling of the potential in the explored range. We noticed, however, that the position of the first peak was very sensitive to the water content of the solvent, an aspect that will be discussed later on. Figure 1 shows typical cyclic voltammetry curves for the oxidation of $C_2O_4^{2-}$ in DMF. The voltammograms, corresponding to two quite different scan rates, illustrate that when v is increased, the second oxidation peak decreases significantly relative to the first. Neither of the two peaks displayed any trace of reversibility at the maximum scan rate employed, 200 V s^{-1}. Similar behavior was observed in MeCN, although the second-to-first peak ratio was found to be slightly smaller compared with DMF, under otherwise identical conditions.

Figure 2 shows the dependence of the peak current (i_p) of the first peak on v. The plot is given in the form of $i_p/(\alpha v)^{1/2}$ to take into account both the effect of v on the diffusion rate and to minimize the potential dependence of α (see below). The plot shows that the normalized current increases significantly with v. This increase is in agreement with the occurrence of a parent–child reaction, i.e. of a reaction between an electrogenerated species and

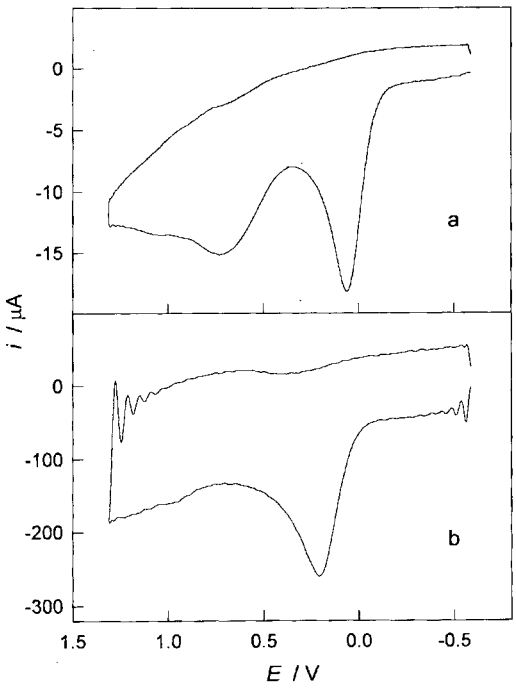

Fig. 1. Cyclic voltammetry curves for the oxidation of 1.0 mM $C_2O_4^{2-}$ in DMF–0.1 M Et_4NClO_4 at a glassy carbon electrode. Scan rate: 0.1 V s^{-1}, curve a; 10 V s^{-1}, curve b.

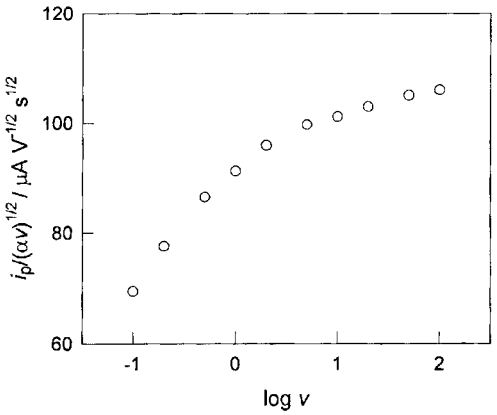

Fig. 2. Dependence of the current function $i_p/(\alpha v)^{1/2}$ on log v for the oxidation of 1.0 mM $C_2O_4^{2-}$ in DMF–0.1 M Et_4NClO_4 at a glassy carbon electrode.

Table 1. Cyclic voltammetric data for the oxidation of oxalate in DMF and MeCN containing 0.1 M Et_4NClO_4 at the glassy carbon electrode. $T = 25$ °C.

Solvent	v/ V s^{-1}	E_p/ V	$\Delta E_{p/2}$/ mV	α^a	$(\partial E_p/\partial \log v)$/ mV $decade^{-1}$	α^b
DMF	0.1	0.046	84	0.57	80.9	0.37
	1.0	0.123	96	0.50		
	10	0.196	104	0.46		
MeCN	0.1	0.202	111	0.43	73.7	0.40
	1.0	0.273	127	0.38		
	10	0.343	140	0.34		

[a]From $\Delta E_{p/2} = 1.857\ RT/F\alpha$. [b]From $\partial E_p/\partial \log v = 1.15\ RT/F\alpha$.

the starting material.[26] Because of the resulting partial deactivation of the starting material, which becomes non-electroactive at the working potentials, this type of reaction is characterized by an apparent number of exchanged electrons that is less than expected on the basis of the electrode stoichiometry. However, provided the timescale of the experiment is short enough, the effect of parent–child reactions can be minimized. This is accomplished by increasing v, as shown in Fig. 2. Moreover, these reactions are bimolecular processes and thus are sensitive to concentration. This is illustrated by Fig. 3, which shows how, at a given scan rate, an increase of the analytical concentration C^* causes a decrease of

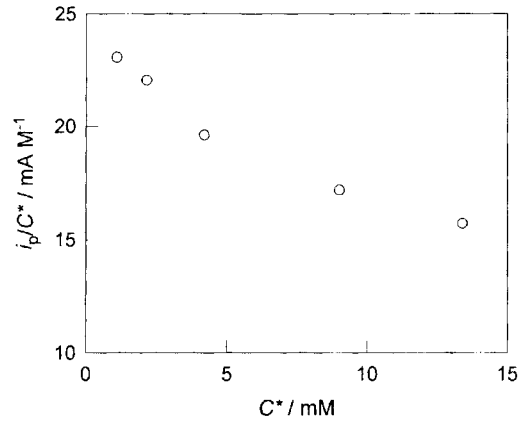

Fig. 3. Dependence of the current function i_p/C^* on log C^* for the oxidation of $C_2O_4^{2-}$ in DMF–0.1 M Et_4NClO_4 at a glassy carbon electrode. Scan rate = 0.2 V s^{-1}.

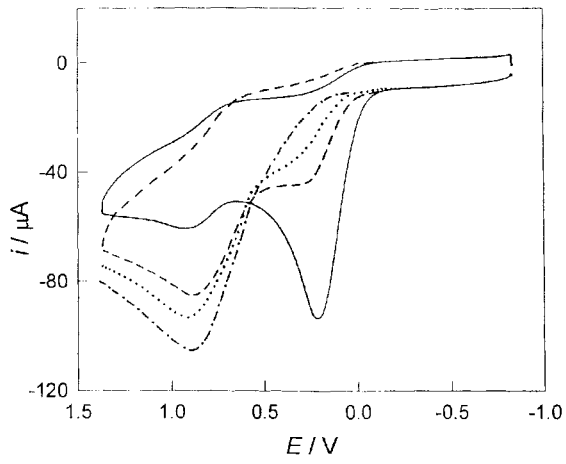

Fig. 4. Cyclic voltammetry curves for the oxidation of 2.0 mM $C_2O_4^{2-}$ in MeCN–0.1 M Et_4NClO_4 at a glassy carbon electrode, obtained in the absence (———) or in the presence of CO_2: [CO_2] = 2.1 mM (– – –); [CO_2] = 10.2 mM (·····); [CO_2] = 280 mM (· – · – ·). Scan rate = 0.2 V s^{-1}.

the ratio i_p/C^*. The parent–child reaction can be outrun, in principle, if C^* is rendered small enough.

Coulometric measurements were carried out at a constant potential just beyond the first voltammetric peak by using both platinum and glassy carbon electrodes. Electrolysis of a 10^{-2} M solution of the oxalate salt, in either DMF or MeCN, required ca. 2 F mol^{-1}, in agreement with the data previously reported on the formation of two CO_2 molecules per oxalate ion,[15b,c] as shown in eqn. (4).

$$C_2O_4^{2-} - 2\,e \rightarrow 2\,CO_2 \qquad (4)$$

Apparently, this is in contrast with the occurrence of a parent–child reaction on the much shorter voltammetric timescale. However, such an experimental outcome is in agreement with the deactivation reaction being reversible. Since the electrode process leads to CO_2, the reaction of oxalate with CO_2 to form an adduct was readily considered to be the most likely process. This was expected to lead to stabilization of the oxalate anion, thus causing its oxidation to occur at more positive potentials. Figure 4 shows the effect of dissolved CO_2 on the electrochemical oxidation of $C_2O_4^{2-}$. The increase of the CO_2 concentration causes a dramatic effect on the relative height of the two peaks (in either DMF or MeCN): while the first oxidation peak decreases until its disappearance at high CO_2 concentrations, the second one increases to form a well-developed peak (at saturation and 0.1 V s^{-1}, E_p is 0.76 and 0.87 V in DMF and MeCN, respectively). The latter has a similar height to that of the first peak in the absence of CO_2, although it is broader. It is noteworthy that, when the solution is purged of CO_2 (by bubbling argon for ca. 20 min), the original voltammetric response of $C_2O_4^{2-}$ is restored. All these observations indicate that the reaction taking place between CO_2 and the oxalate ion is reversible [eqn. (5)] and leads to the species that is oxidized at the second peak.

$$CO_2 + C_2O_4^{2-} \rightleftharpoons CO_2,C_2O_4^{2-} \qquad (5)$$

Comparison with the curve obtained in a solution containing $HC_2O_4^-$ (at 0.1 V s^{-1}, E_p is 0.94 and 1.04 V in DMF and MeCN, respectively) allowed us to exclude this as the species responsible for second peak of $C_2O_4^{2-}$. This had to be checked because the second peak had previously been attributed to the oxidation of $HC_2O_4^-$ to yield CO_2.[15d] The monoanion was assumed to be formed by reaction of $C_2O_4^{2-}$ with the residual water in the solvent [eqn. (6)]. This equilibrium was supposed to be driven to the right thanks to trapping of OH^- by the carbon dioxide produced during the oxidation of $C_2O_4^{2-}$ at the first peak [eqn. (7)].

$$C_2O_4^{2-} + H_2O \rightleftharpoons HC_2O_4^- + OH^- \qquad (6)$$

$$CO_2 + OH^- \rightleftharpoons HCO_3^- \qquad (7)$$

On the other hand, equilibrium (6) is quite unfavorable: the equilibrium constant was calculated to be 8×10^{-16} by using the pK_a values of H_2O and of $HC_2O_4^-$ in DMF (31.7 and 16.6, respectively).[27] In addition, the voltammetric pattern of $C_2O_4^{2-}$ in a CO_2-saturated solvent is unaffected by the presence of H_2O up to 1 M concentration. In particular, no tendency to form an oxidation peak coincident with that of the monoanion was observed.

On these grounds, the oxidation of $C_2O_4^{2-}$ was analyzed from the point of view of the kinetics of the heterogeneous electron transfer. The first peak potential shifts toward more positive values when the scan rate is increased and a linear variation of E_p as a function of log v was observed in both solvents. The slopes of the E_p–log v plots (Table 1) are large, pointing to the heterogeneous electron transfer as the rate-determining step. The transfer coefficient was calculated from these slopes and also from the half-peak width ($\Delta E_{p/2}$) values (Table 1), according to the equations valid for an irreversible electron transfer.[21] For both solvents an import-

ant observation on the electron transfer mechanism is that the α value obtained from the $\Delta E_{p/2}$ measurements decreases when v increases. In particular, since upon increasing v the irreversible voltammetric peak shifts toward more positive potentials and broadens, cyclic voltammetry indicates that α decreases when E becomes more positive. As a consequence, the Butler–Volmer kinetic law,[21] in which α is assumed to be constant at any E value, cannot be used to describe satisfactorily the electrode process. The heterogeneous electron transfer was thus studied by using a more sophisticated approach, the convolution analysis.[20c,22]

The convolution analysis is based on a series of steps in which background-subtracted cyclic voltammograms are first treated to transform the real current i into a convoluted current I. I is then used together with i to obtain the potential dependence of the heterogeneous electron transfer rate constant, k_{het}, without the need of defining the electron transfer rate law. Provided the electrode process is irreversible, eqn. (8) is used

$$\ln k_{het} = \ln D^{1/2} - \ln\{[I_l - I(t)]/i(t)\} \quad (8)$$

where D is the diffusion coefficient and I_l is the limiting value of I attained when the electrode process becomes diffusion controlled.[22] Afterwards, the potential dependence of k_{het} is analyzed to obtain the corresponding potential dependence of α, through eqn. (9),

$$\alpha = (RT/F)\,\partial \ln k_{het}/\partial E \quad (9)$$

which derives from the fact that α is defined as $\partial\Delta G^{\neq}/\partial\Delta G^{\circ}$, where $\Delta G^{\neq}$ is the free energy of activation and ΔG° the free energy of the reaction. Actually, both k_{het} and α data should be corrected for the effect of the electric double layer. However, apparent data seem to provide a reasonable estimate of the actual parameters,[20c,d] also in view of the preliminary results obtained on the double layer properties of glassy carbon in DMF.[28]

The background-subtracted i–E curves pertaining to the electro-oxidation of $C_2O_4^{2-}$ in anhydrous DMF were thus treated to obtain the corresponding I–E curves. The procedure was carried out for several values of v in the range 0.1–50 V s^{-1} and was repeated in separate experiments by using different samples of $[Bu_4N]_2C_2O_4$ to check the reproducibility of the results. A typical convolution voltammogram is shown in Fig. 5, together with the corresponding linear scan voltammetry. As can be seen the I–E plot does not reach a plateau, as would be expected for an uncomplicated process.[22] Instead, the convoluted curve is peak-shaped. This is for the same reason why the peak in the i–E curve is sharper than a normal diffusion-controlled peak. In fact, the parent–child reaction causes the concentration of $C_2O_4^{2-}$ in the reaction layer to drop with respect to the values expected for an electrode process in which the starting material is destroyed only because of the heterogeneous electron transfer.[26] This effect is less pronounced at high values of v, when the timescale of the experiment is short

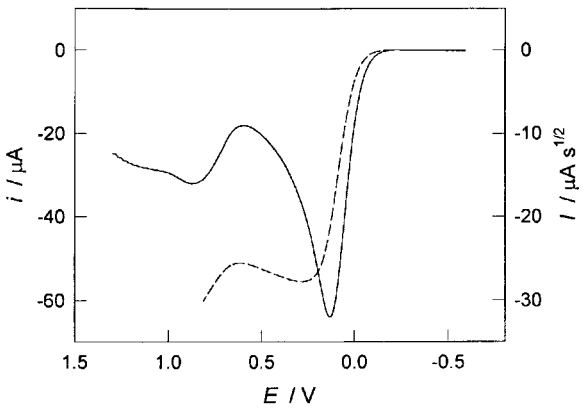

Fig. 5. Convolution (– – –) and background-subtracted voltammetric (———) curves for the oxidation of 1.0 mM $C_2O_4^{2-}$ in DMF–0.1 M Et_4NClO_4 at a glassy carbon electrode. Scan rate = 1 V s^{-1}.

enough that the chemical reaction occurs to only a small extent. This caused the logarithmic analysis, which requires knowledge of the value of I_l [see eqn. (8)], to be more difficult than in other investigations.[20c,d,f,23,29] On the other hand, provided there are no specific heterogeneous effects, it is also true that at any given E the same k_{het} should be obtained, to within error, from measurements performed at different scan rates. In addition, the error on $\ln k_{het}$ due to imprecision on I_l is more pronounced at the E values at which I is larger [eqn. (8)]. We found that a good approach was to start by making a reasonable estimate of I_l,† for each set of I–E data pertaining to the various scan rates. In this way one obtains an initial set of $\ln k_{het}$–E values. By weighting more the less positive E values of each data set, comparison between the different sets allows one to select a better I_l value for each scan rate. By this simple interactive procedure, an overall $\ln k_{het}$–E plot, encompassing all of the employed scan rates, can be obtained. The procedure was carried out separately for different experiments leading to a very good agreement between the correponding sets of data. As already discussed,[20d] this agreement provides an *a posteriori* indication that the ohmic drop correction was properly adjusted in the acquisition of the experimental curves. In fact, improper ohmic-drop compensation leads to both a negative shift and a broadening of the voltammetric curves; in terms of the convolution output, this would result in poor overlap of the $\ln k_{het}$–E plots obtained in the same potential range at different scan rates. The convolution procedure was carried out also for the single peak observed after saturation of the solution with CO_2, i.e. under the conditions in which only the second peak is observable (cf. Fig. 4). The analysis of these experiments was easier than above in that a relatively good plateau

† Since $I_l = nFAD^{1/2}C^*$,[22] where n is the overall electron consumption, it should be independent of the scan rate. In practice, however, the occurrence of the parent–child reaction causes n to vary between 1 and 2 as a function of v.[26] Under these conditions, I_l too is dependent on v.

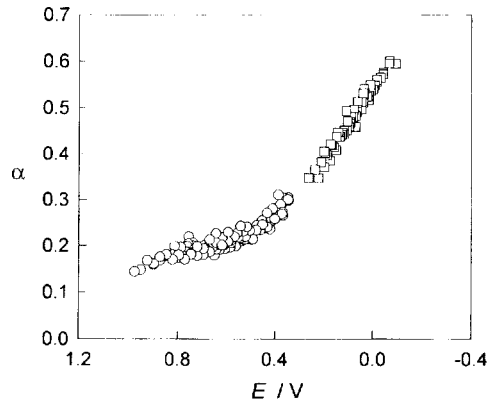

Fig. 6. Potential dependence of the transfer coefficient α for the oxidation of 1.0 mM $C_2O_4^{2-}$ in DMF–0.1 M Et_4NClO_4 at a glassy carbon electrode. The α data pertain to experiments carried out at scan rates in the range 0.1–50 V s^{-1} either in the absence (□) or in the presence of 0.20 M CO_2 (○).

was obtained at any scan rate, the I_l value being independent of the scan rate to within 3%. Derivatization was accomplished by linear regression of the $\ln k_{het}$–E sets within small E intervals (21 to 29 mV). In this way, both linear and non-linear potential dependences of α are detectable.[20c,d] The result of the α analysis, carried out independently for the first and the second peak, is shown by Fig. 6.

Let us consider first the main oxidation peak. In general, the experimental observation of a potential dependence of α, beyond experimental error, suggests that a Marcus-like quadratic activation–driving force relationship may adequately describe the experimental behavior.[20c,30] In fact, the kinetics of both the stepwise [eqns. (10), (11)] and concerted [eqn. (12)] oxidation mechanisms can be described by eqn. (13),

$$C_2O_4^{2-} - e \rightarrow C_2O_4^{\cdot -} \quad (10)$$

$$C_2O_4^{\cdot -} \rightarrow CO_2 + CO_2^{\cdot -} \quad (11)$$

$$C_2O_4^{2-} - e \rightarrow CO_2 + CO_2^{\cdot -} \quad (12)$$

$$\Delta G^{\neq} = \Delta G_0^{\neq}\left(1 + \frac{\Delta G^{\circ}}{4\Delta G_0^{\neq}}\right)^2 \quad (13)$$

where $\Delta G_0^{\neq}$ is the intrinsic barrier, i.e. the activation free energy at zero driving force. Whereas the intrinsic barrier of a simple outer sphere electron transfer [such as eqn. (10)] is ruled by solvent and intramolecular reorganization energies, λ ($4\Delta G_0^{\neq} = \lambda$), that of a concerted dissociative process [such as eqn. (12)] also contains a significant contribution from the BDE, i.e. the dissociation energy of the breaking bond ($4\Delta G_0^{\neq} = BDE + \lambda$).[17]

Provided only one electron transfer mechanism, obeying the simple rate–free energy law (13), takes place upon electro-oxidation of the substrate in a certain potential range, the transfer coefficient α is dependent upon the driving force and thus the applied potential E according to eqn. (14), where the effect of the double layer has been neglected. Equation (14) contains three aspects that are worth noting. First, $\alpha = 0.5$ when $E = E^{\circ}$. Second, α is a linear function of E. Third, the slope is inversely proportional to the intrinsic barrier.

$$\alpha = 0.5 - \frac{F}{8\Delta G_0^{\neq}}(E - E^{\circ}) \quad (14)$$

The fact that most of the α data are close and some of them even larger than 0.5 is *per se* a good, though qualitative, indication that the dissociative electron transfer mechanism is stepwise.[17] However, on the basis of the experimentally determined potential dependence of α, a more quantitative analysis can be carried out. The experimental α data, which are satisfactorily linear in the investigated potential range (Fig. 6), allow us to estimate both the standard potential for oxalate oxidation, +0.06 V (mostly because of the double layer approximation, the uncertainty is estimated to be ±0.1 V), and the intrinsic barrier, 3.7 kcal mol^{-1}. The latter figure corresponds to an overall reorganization energy of 14.8 kcal mol^{-1}. This value can now be compared with the solvent reorganization energy, λ_s, which can be calculated by using either the Marcus approach [$\lambda_s = e^2(1/\varepsilon_{op} - 1/\varepsilon_s)/4r$], where e is the charge of the electron and ε_{op} and ε_s are the high frequency and static dielectric constants of the solvent) or the empirical equation $\lambda_s = 55.7/r$, as previously discussed.[20c] The radius r of oxalate was roughly estimated by using the experimentally determined diffusion coefficient of oxalate (determined through the analysis of the I_l values) and the Stokes equation, to be 2.6 Å (a bit larger than expected, most likely because of some ion-pairing with the tetraethylammonium cations of the electrolyte). The solvent reorganization energy λ_s values can thus be calculated by using the above equations to be 14.8 and 21.5 kcal mol^{-1}, respectively. By comparison of the above values it should be concluded that λ_s is the most important energetic factor ruling the kinetics of the heterogeneous process and, most important, that the electrooxidation of oxalate is a stepwise dissociative electron transfer [eqns. (10) and (11)]. More careful analysis of the data, however, is required to assess the mechanism.

An estimate of the standard potential for the corresponding concerted dissociative oxidation of $C_2O_4^{2-}$ [eqn. (12)] can be made by using the appropriate thermochemical cycle,[31] through eqn. (15).

$$E^{\circ}_{CO_2,CO_2^{\cdot -}/C_2O_4^{2-}} = BDFE/F + E^{\circ}_{CO_2/CO_2^{\cdot -}} \quad (15)$$

where BDFE is the C–C bond dissociation free energy in the oxalate anion. Whereas the standard potential for CO_2 reduction has been estimated to be −2.21 V,[16a,32] the BDFE value for $C_2O_4^{2-}$ cannot be estimated because of the lack of available thermochemical data. The standard formation enthalpies of the radical $^{\cdot}CO_2H$ (−52.7 kcal mol^{-1}) and oxalic acid (−175.0 kcal mol^{-1}) can be used,[33] together with an entropy correction of 6 kcal mol^{-1},[20c] to estimate the C–C BDFE of oxalic acid to be 63.6 kcal mol^{-1}. This value can be taken

as the maximum value of the BDFE of $C_2O_4^{2-}$ and thus [eqn. (15)] poses a maximum positive limit to $E^\circ_{CO_2,CO_2^{\cdot-}/C_2O_4^{2-}}$ of 0.55 V. This potential value is much more positive than that determined experimentally, 0.06 V, and also to the position of the peak at any scan rate employed. On the other hand, one might assume that the experimentally determined value is that of a concerted dissociative process. In this case, the BDFE of $C_2O_4^{2-}$ would be 52.2 kcal mol^{-1}. In principle, this might be attributed to a decrease of the bond strength on going from oxalic acid to its dianion. Even under this assumption, however, and according to the Savéant theory,[17] the intrinsic barrier and the overall λ would be no less than 16.8 and 67 kcal mol^{-1}, respectively (these are minimum values because we used the smallest values of both BDFE and λ_s and neglected any inner reorganization contribution to λ). On one hand, however, such a high value would mean a large activation overpotential with the result of causing the experimental voltammetric peak to appear at a potential much more positive than that of E°. On the other hand, it would also mean that $\partial\alpha/\partial E \leqslant 0.17$ V^{-1}, a slope much smaller than that determined experimentally, 0.78 V^{-1}. The latter value, however, is not corrected for the double layer effect. In fact, preliminary data on the double layer at the glassy carbon DMF–Bu_4NClO_4 interface point to a potential of zero charge of 0.19 V vs. SCE.[28] Although the electrolyte is not the same as in the present study, it is reasonable to expect that, for the DMF–Et_4NClO_4 system, the variation of the diffuse-layer potential in the potential region where the apparent α values were determined is also significant. This source of uncertainty reduces the reliability of the experimental intrinsic barrier computed through eqn. (14).

The role of the intramolecular reorganization energy λ_i can be estimated from the $\ln k_{het}$–E data obtained through eqn. (8). By use of the results obtained for $E = E^\circ$, the apparent value of the heterogeneous standard rate constant, k°, was calculated to be 8.1×10^{-3} cm s^{-1}. The reorganization energy was then calculated to be 32.3 kcal mol^{-1} by using the Eyring equation and an adiabatic pre-exponential factor $Z = (RT/2\pi M)^{1/2} = 6.7 \times 10^3$ cm s^{-1}. Taking into account the above estimates of λ_s, this would indicate that indeed λ_i accounts for 30–50% of λ. Nevertheless, even this latter estimate provides a λ value much smaller than the minimum value expected for a concerted dissociative electron transfer. In conclusion, there is little doubt that the oxidation of the oxalate anion proceeds according to the stepwise mechanism given by eqns. (10) and (11).

A final comment concerns why λ_i amounts to 11–18 kcal mol^{-1}. By using a thermochemical cycle, it is possible to relate the difference between the BDFE of $C_2O_4^{2-}$ and that of $C_2O_4^{\cdot-}$, $BDFE_{(\cdot-)}$, to the estimated standard potentials pertaining to the $CO_2/CO_2^{\cdot-}$ and $C_2O_4^{\cdot-}/C_2O_4^{2-}$ couples [eqn. (16)]:

$$BDFE - BDFE_{(\cdot-)} = F(E^\circ_{C_2O_4^{\cdot-}/C_2O_4^{2-}} - E^\circ_{CO_2/CO_2^{\cdot-}}) \quad (16)$$

In this way, independently of the actual values of BDFE and $BDFE_{(\cdot-)}$, it appears that upon formation of $C_2O_4^{\cdot-}$ the C–C bond weakens by ca. 50 kcal mol^{-1} with respect to $C_2O_4^{2-}$. This effect is very similar to that found by studying the stepwise dissociative electron transfer to diaryl disulfides;[23b] for these compounds, experimental data and theoretical calculations concur to indicate that the observed large λ_i is caused by significant stretching of the S–S bond in the transition state. Although this could also be possible in the present case, it seems more likely that for oxalate the inner reorganization component is mostly determined by substantial increase of the O–C–O angle upon formation of the $COO^\cdot$ moiety.

Analysis of the kinetic data pertaining to the single peak observed upon saturation of the solution with CO_2 is more challenging. In fact, Fig. 6 shows that there is no linear trend in the pertinent α data. On the other hand, as stated above, a linear trend would be expected if only one electron transfer mechanism takes place at the electrode. This cannot be the case if we consider equilibrium (5). Even though the equilibrium lies on the right, some free oxalate is still present (Fig. 4, e.g., illustrates how high the CO_2 concentration must be in order to suppress the first peak completely) and thus oxidizable at the base of the voltammetric wave. Moreover, oxidation of the free oxalate is liable to induce further dissociation of the adduct, in particular at low scan rates and thus on the longest timescales employed. In fact, Figs. 1–3 witness the fact that the rate constant for the formation of the adduct cannot be very large, because at the highest scan rates the chemical complication is negligible. That the standard potential for oxidation of the oxalate–CO_2 adduct is more positive than that for the free oxalate anion (as is E_p) is reasonable because of the stabilizing interaction. This means that, as the potential is rendered more positive, direct oxidation of the adduct tends to become the only oxidation process. Therefore, the α data obtained through analysis of the second peak are not pure but apparent α data, pertaining to an observed k_{het} that is the sum of two parallel contributions.

This kind of competition between distinct electrode processes having different E° and (possibly) intrinsic barriers is thus driven by the applied potential. In this light, the two sets of α data shown in Fig. 6 pertain to the same overall curve. The α data collected by studying the second peak would provide the zone of transition between pure oxidation of free $C_2O_4^{2-}$ and pure oxidation of its CO_2 adduct. This effect of E on α is similar, though conceptually not equal, to that recently proposed for the reduction of *tert*-butyl 4-cyanoperbenzoate[20d] and now extended to other perbenzoates.[34] The main difference is that whereas in the case of reduction of perbenzoates and also of some sulfur compounds[35] the observed transition (in terms of α or of the electron transfer rate constant) is a transition between two mechanisms, concerted and stepwise, the transition proposed for oxalate oxidation would concern the actual species undergoing

the heterogeneous electron transfer and not the type of mechanism. Unfortunately, in the case of the second peak of oxalate, no linear region in the α–E plot could be experimentally reached on the positive side of the E range; this prevents further analysis of the data to obtain information on the kinetic parameters characterizing the oxidation of the adduct. It seems likely, however, that even the oxidation of the adduct obeys a stepwise mechanism similar to that followed by the free oxalate.

The voltammetric behavior of $C_2O_4^{2-}$ is highly influenced by the presence of acids in solution. Addition of 1 equivalent of $HClO_4$ causes the disappearance of both oxidation peaks of the $C_2O_4^{2-}$ ion. They are replaced by a new irreversible oxidation peak that is more positive by ca. 0.2 V than the second oxidation peak of $C_2O_4^{2-}$ (Fig. 7, dashed line). As mentioned above, this peak is attributed to the oxidation of the hydrogenoxalate ion $HC_2O_4^-$ formed by reaction of $C_2O_4^{2-}$ with $HClO_4$. Addition of another equivalent of $HClO_4$ leads to the disappearance of this peak because of formation of oxalic acid. Under these conditions, no electroactivity is detectable in the available potential window. When a weak acid such as trifluoroethanol (TFE), pK_a (DMF)= 24.1,[2a,b] is added to a solution of $C_2O_4^{2-}$, in either DMF or MeCN, the first oxidation peak shifts toward more positive potentials while the second one decreases and disappears when the TFE concentration is ca. 1 M. In addition, the first oxidation peak becomes much broader (at 0.2 V s^{-1}, e.g., α decreases from 0.55, in the absence of TFE, to 0.30, after TFE addition), pointing to some change in the electrode mechanism. Addition of H_2O to a solution of $C_2O_4^{2-}$ causes a slight increase and a positive shift of the first peak, E_p, depending markedly on the water concentration (Fig. 7). No oxidation peak attributable to $HC_2O_4^-$ was observed in the presence of H_2O, even at molar concentrations. Unlike the effect of strong proton donors such as $HClO_4$, the observed positive shift of the first peak points to a hydrogen-bonding stabilization brought about by weak proton donors, such as TFE and H_2O. Figure 8 shows the effect of the concentration of either TFE or H_2O on the potential of the first peak relative to the E_p value measured in the absence of added acids, $E_{p,0}$. In this framework, the large shift caused by TFE addition would indicate that TFE is a better hydrogen-bonding donor compared with H_2O. This would be expected on the basis of a simple pK_a comparison.[36]

The two slopes into which both the DMF and MeCN E_p–$E_{p,0}$ versus log[H_2O] plots can be broken may be used to carry out a rough calculation to shed some light on the interaction between oxalate and water. Their reaction may be written as eqn. (17).

$$C_2O_4^{2-} + qH_2O \rightleftharpoons [C_2O_4(H_2O)_q]^{2-} \qquad (17)$$

In the hypothesis that, in the presence of H_2O, the species undergoing oxidation is still the free oxalate ion, the consequence of equilibrium (17) is to force the oxidation to take place at more positive potentials than in the absence of H_2O. This would be in agreement with the pattern shown by Fig. 7. From a quantitative point of view, the equilibrium constant K of reaction (17) and the coordination number q can be calculated by applying the treatment previously derived for the analogous system in which a metal cation, in equilibrium with its complex with a certain ligand (in large excess with respect to the cation), undergoes a slow heterogeneous electron transfer.[37] In this framework, the shift of the oxidation peak of $C_2O_4^{2-}$ can be related to K and H_2O concentration according to eqn. (18),

$$E_p - E_{p,0} = -\frac{RT}{2\alpha F}\ln\frac{D}{D'} + \frac{RT}{\alpha F}\ln K + q\frac{RT}{\alpha F}\ln[H_2O] \qquad (18)$$

where $E_{p,0}$ and E_p are the peak potentials for the oxidation of oxalate measured in the absence and in the presence of H_2O, respectively, and D' is the diffusion

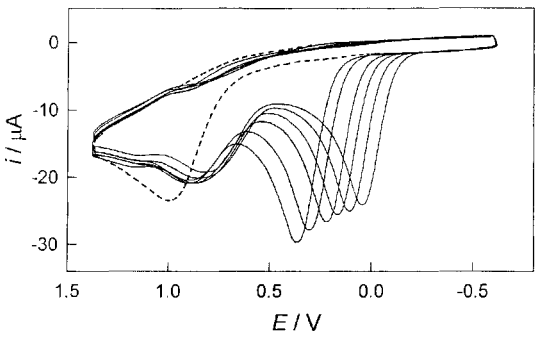

Fig. 7. Cyclic voltammetry curves for the oxidation of 1.1 mM $C_2O_4^{2-}$ in DMF–0.1 M Et_4NClO_4 in the presence of H_2O (solid lines). From right to left: [H_2O]=0, 0.1, 0.2, 0.4, 0.8, and 1.2 M. The dashed line is the curve for the oxidation of 1.1 mM $HC_2O_4^-$. Glassy carbon electrode, 0.2 V s^{-1}.

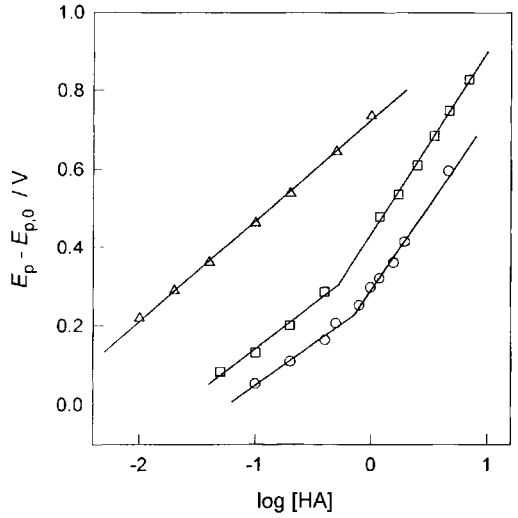

Fig. 8. Dependence of the first peak potential for the oxidation of 1.1 mM $C_2O_4^{2-}$ on the molar concentration of H_2O (□, MeCN; ○, DMF) and TFE (△, DMF). The shift is expressed relative to the peak potential, $E_{p,0}$, measured in the absence of HA. Glassy carbon electrode, 0.2 V s^{-1}.

coefficient of the water–oxalate adduct. The fact that, for both DMF and MeCN, the plot $E_p - E_{p,0}$ versus $\log[H_2O]$ displays two different slopes (Fig. 8) is consistent with a variation of q and thus with two different adducts prevailing in solution depending on the concentration of H_2O. The calculation was carried out using the same α value independently of the water concentration (at 0.2 V s^{-1}, α is 0.55 and 0.41 in DMF and MeCN, respectively). The values of q calculated in this way from the slopes of the two linear segments are 2 and 4, in either solvent. The stability constants for the two adducts can be calculated by using eqn. (18). Although the diffusion coefficients of the two adducts could not be calculated, we may reasonably assume that the ratio D/D' does not differ too much from 1 [even if $D = 1.5D'$, the first term of the right-hand side of eqn. (18) is only -10 mV] and the corresponding term can be neglected. The calculated values of K for the 2:1 and 4:1 adducts are 2.7×10^2 and 5.0×10^2, in DMF, and 1.9×10^3 and 1.0×10^4, in MeCN, respectively. The uncertainty of the K values is estimated to be 20–25%. Both the q and K values seem to be reasonable. For example, for moderately large water concentrations, a q value of 2 reflects that expected for a favorable hydrogen-bonding interaction leading to two six-membered systems H–O–H···O–C–O. On the other hand, although the capability of the two solvents to solvate the oxalate dianion should be similar (according to the acceptor numbers of MeCN and DMF), smaller K values for DMF are in line with DMF being superior to MeCN as a hydrogen-bond acceptor.[38]

Conclusions

This is the first study in which the oxidation of a carboxylate has been studied in detail from the point of view of the concerted-versus-stepwise nature of the dissociative electron transfer mechanism. Oxalate dianion was chosen because of its peculiar structure and overall stoichiometry [eqn. (4)] in an effort to obtain evidence for a concerted dissociative oxidation, to parallel the increasing literature on the corresponding dissociative reductions.[17–20] Instead, the voltammetric and convolution analyses led to unequivocal evidence for a stepwise mechanism. Although the oxidation of oxalate dianion is quite irreversible, the standard potential for the formation of the corresponding radical anion [eqn. (10)] could be evaluated to be 0.06 V vs. SCE in DMF. This result is worth noting because it seems to be the first non-thermochemical estimate of the standard potential for the oxidation of a carboxylate ion.

Besides the C–C cleavage reaction [eqn. (11)] and the subsequent oxidation of the carbon dioxide radical anion, other reactions may take place in solution depending on the timescale of the experiment and the presence of acidic species. The CO_2 molecules released during the oxidation of $C_2O_4^{2-}$ interact with the starting material itself with the formation of an adduct that can be oxidized at more positive potential values. As a consequence, when the potential is positive enough, both the free and the complexed oxalate ions compete in the overall electrooxidation. This is also supported by the non-linear potential dependence of α observed in this E region, providing an example of mechanism transition, although different from those found by studying the dissociative reduction of peroxides[20d,34] and sulfur compounds.[35]

Besides these theoretical aspects, there are some practical ones that derive from the study of the effect of mild acids on oxalate oxidation. The anodic oxidation of oxalate to CO_2 has been previously suggested to be an innocuous reaction suitable to be employed as a sacrificial anodic process to be paired in cathodic electrosyntheses in undivided cells.[15a,b] Obviously, in these cells, the actual oxidation potential of the desired electrogenerated reduction product must be more positive than that of the anodic depolarizer, e.g. oxalate, to ensure selective oxidation of the latter. The presence of H_2O in aprotic solvents, however, causes considerable positive shifts of the actual potential for the oxidation of $C_2O_4^{2-}$. Use of oxalate oxidation as a sacrificial anodic process in undivided cells without attention to this effect may thus lead to undesirable results, such as large cell voltages or partial destruction of the reduction product. For similar reasons, the potential shift caused by the presence in solution of hydrogen-bonding species is liable to interfere in theoretical studies concerning the electro-oxidation mechanism of anions. In particular, potential shifts of this type may affect the determination of the apparent standard potential of a dissociative oxidation. This would affect also the reliability of the use of eqn. (15) to evaluate the solution BDFE values, an approach that we have recently used with success in the field of the reduction of peroxides.[20c]

Acknowledgements. This work was financially supported by the Consiglio Nazionale delle Ricerche, the Ministero dell'Università e della Ricerca Scientifica e Tecnologica.

References

1. Vijh, A. K. and Conway, B. E. *Chem. Rev. 67* (1967) 623.
2. Fry, A. J. *Synthetic Organic Electrochemistry,* 2nd ed., Wiley, New York 1989.
3. Schafer, H. J. *Top. Curr. Chem. 152* (1990) 91.
4. Torii, S. and Tanaka, H. In: Lund, H. and Baizer, M. M., Eds., *Organic Electrochemistry*, 3rd ed., Marcel Dekker, New York 1991, pp. 535–579.
5. (a) Andrieux, C. P., Gonzalez, F., Savéant, J.-M. *J. Am. Chem. Soc. 119* (1997) 4292; (b) Klocke, E., Matzeit, A., Gockeln, M. and Schäfer, H. J. *Chem. Ber. 126* (1993) 1623; (c) Vassiliev, Yu. B. and Grinberg, V. A. *J. Electroanal. Chem. 308* (1991) 1; (d) Hawkes, G. E., Utley, J. H. P. and Yates, G. B. *J. Chem. Soc., Perkin Trans. 2* (1976) 1709; (e) Muck, D. L. and Wilson, E. R. *J. Electrochem. Soc. 117* (1970) 1358; (f) Reichenbacher, P. H., Morris, M. D. and Skell, P. S. *J. Am. Chem. Soc. 90* (1968) 3432; (g) Rand, L. and Mohar, A. F. *J. Org. Chem. 30* (1965) 3156.
6. (a) Cervino, R. M., Triaca, W. E. and Arvia, A. J. *J. Electroanal. Chem. 172* (1984) 255; (b) Coleman, J. P.,

Lines, R., Utley, J. H. P. and Weedon, B. C. L. *J. Chem. Soc., Perkin Trans. 2* (1974) 1064.
7. (a) Kraeutler, B. and Bard, A. J. *J. Am. Chem. Soc. 100* (1978) 2239; (b) Kraeutler, B. and Bard, A. J. *J. Am. Chem. Soc. 100* (1978) 4903; (c) Reichenbacher, P. H., Liu, M. Y.-C. and Skell, P. S. *J. Am. Chem. Soc. 90* (1968) 1816; (d) Conway, B. E. and Vijh, A. K. *Electrochim. Acta 12* (1967) 102.
8. (a) Eberson, L. *Acta Chem. Scand. 17* (1963) 2004; (b) Eberson, L. *Electrochim. Acta 12* (1967) 1473.
9. Eberson, L. *Acta Chem. Scand., Ser. B 36* (1982) 533.
10. For example, see: Steffen, L. K., Glass, R. S., Sabahi, M., Wilson, G. S., Schöneich, C., Mahling, S. and Asmus, K.-D. *J. Am. Chem. Soc. 113* (1991) 2141.
11. (a) Chateauneuf, J., Lusztyk, J. and Ingold, K. U. *J. Am. Chem. Soc. 109* (1987) 897; (b) Chateauneuf, J., Lusztyk, J. and Ingold, K. U. *J. Am. Chem. Soc. 110* (1988) 2877; (c) Chateauneuf, J., Lusztyk, J. and Ingold, K. U. *J. Am. Chem. Soc. 110* (1988) 2886; (d) Korth, H.-G., Müller, W., Lusztyk, J. and Ingold, K. U. *Angew. Chem., Int. Ed. Engl. 28* (1989) 183.
12. (a) Pincock, J. A. *Acc. Chem. Res. 30* (1997) 43; (b) Hilborn, J. W. and Pincock, J. A. *J. Am. Chem. Soc. 113* (1991) 2683; (c) Falvey, D. E. and Schuster, G. B. *J. Am. Chem. Soc. 108* (1986) 7419.
13. (a) Bockman, T. M., Hubig, S. M. and Kochi, J. K. *J. Am. Chem. Soc. 118* (1996) 4502; (b) Bockman, T. M., Hubig, S. M. and Kochi, J. K. *J. Org. Chem. 62* (1997) 2210.
14. (a) Morris, M. D. *J. Electroanal. Chem. 8* (1964) 350; (b) Johnson, J. W., Wroblowa, H. and Bockris, J. O'M. *Electrochim. Acta 9* (1964) 639; (c) Anson, F. C. and Schultz, F. A. *Anal. Chem. 35* (1963) 1114; (d) Giner, J. *Electrochim. Acta 4* (1961) 42; (e) Lingane, J. J. *J. Electroanal. Chem. 1* (1960) 379.
15. (a) Pletcher, D. and Girault, J. T. *J. Appl. Electrochem. 16* (1986) 791; (b) Engels, R., Smit, C. J. and van Tilborg, W. J. M. *Angew. Chem. Suppl.* (1983) 691; (c) Chang, M.-M., Saji, T. and Bard, A. J. *J. Am. Chem. Soc. 99* (1977) 5399; (d) Jacobsen, E. and Sawyer, D. T. *J. Electroanal. Chem. 16* (1968) 361.
16. (a) Gennaro, A., Isse, A. A., Savéant, J.-M., Severin, M. G. and Vianello, E. *J. Am. Chem. Soc. 118* (1996) 7190; (b) Gennaro, A., Isse, A. A., Severin, M. G., Vianello, E., Bhugun, I. and Savéant, J.-M. *J. Chem. Soc., Faraday Trans. 92* (1996) 3963.
17. Savéant, J.-M. In: Mariano, P. S., Ed., *Advances in Electron Transfer Chemistry*, JAI Press, Greenwich, CT 1994, Vol. 4, p. 53.
18. (a) Savéant, J.-M. *Adv. Phys. Org. Chem. 26* (1990) 1; (b) Savéant, J.-M. *Acc. Chem. Res. 26* (1993) 455.
19. (a) Daasbjerg, K., Pedersen, S. U. and Lund, H. *Acta Chem. Scand. 45* (1991) 424; (b) Lund, H., Daasbjerg, K., Lund, T. and Pedersen, S. U. *Acc. Chem. Res. 28* (1995) 313.
20. (a) Workentin, M. S., Maran, F. and Wayner, D. D. M. *J. Am. Chem. Soc. 117* (1995) 2120; (b) Kjær, N. T. and Lund, H. *Acta Chem. Scand. 49* (1995) 848; (c) Antonello, S., Musumeci, M., Wayner, D. D. M. and Maran, F. *J. Am. Chem. Soc. 119* (1997) 9541; (d) Antonello, S. and Maran, F. *J. Am. Chem. Soc. 119* (1997) 12595; (e) Workentin, M. S. and Donkers, R. L. *J. Am. Chem. Soc. 120* (1998) 2664; (f) Donkers, R. L. and Workentin, M. S. *J. Phys. Chem. B 102* (1998) 4061; (g) Donkers, R. L., Maran, F., Wayner, D. D. M. and Workentin, M. S. *J. Am. Chem. Soc. 121* (1999) 7239.
21. Bard, A. J. and Faulkner, L. R. *Electrochemical Methods, Fundamentals and Applications*, Wiley, New York 1980.
22. Imbeaux, J. C. and Savéant, J.-M. *J. Electroanal. Chem. 44* (1973) 169.
23. (a) Antonello, S. and Maran, F. *J. Am. Chem. Soc. 120* (1998) 5713; (b) Daasbjerg, K., Jensen, H., Benassi, R., Taddei, F., Antonello, S., Gennaro, A. and Maran, F. *J. Am. Chem. Soc. 121* (1999) 1750; (c) Severin, M. G., Arévalo, M. C., Maran, F. and Vianello, E. *J. Phys. Chem. 97* (1993) 150.
24. Vogel, A. I. *Textbook of Quantitative Inorganic Analysis*, 2nd ed., Longman, Green and Co., London 1955, p. 275.
25. Gennaro, A., Isse, A. A. and Vianello, E. *J. Electroanal. Chem. 289* (1990) 203.
26. (a) Maran, F., Roffia, S., Severin, M. G. and Vianello, E. *Electrochim. Acta 35* (1990) 81; (b) Arévalo, M. C., Farnia, G., Severin, M. G. and Vianello, E. *J. Electroanal. Chem. 220* (1987) 201.
27. (a) Maran, F., Celadon, D., Severin, M. G. and Vianello, E. *J. Am. Chem. Soc. 113* (1991) 9320; (b) Bordwell, F. G. *Acc. Chem. Res. 21* (1988) 456; (c) Olmstead, W. N., Margolin, Z. and Bordwell, F. G. *J. Org. Chem. 45* (1980) 3295; (d) Gavrilov, A. V., Kurmaeva, A. I., Tret'yakova, A. Ya., Barabanov, V. P. and Kitsya, V. P. *Zh. Anal. Khim. 34* (1979) 771.
28. Arévalo, M. C. and Maran, F. *Unpublished data.*
29. (a) Savéant, J.-M. and Tessier, D. *J. Electroanal. Chem. 65* (1975) 57; (b) Savéant, J.-M. and Tessier, D. *J. Phys. Chem. 81* (1977) 2192; (c) Savéant, J.-M. and Tessier, D. *J. Phys. Chem. 82* (1978) 1723; (d) Klinger, R. J. and Kochi, J. K. *J. Am. Chem. Soc. 103* (1981) 5839; (e) Amatore, C., Savéant, J.-M. and Tessier, D. *J. Electroanal. Chem. 146* (1983) 37; (f) Andrieux, C. P., Gallardo, I., Savéant, J.-M. and Su, K. B. *J. Am. Chem. Soc. 108* (1986) 638; (g) Petersen, R. A. and Evans, D. H. *J. Electroanal. Chem. 222* (1987) 129; (h) Bond, A. M., Mahon, P. J., Maxwell, E. A., Oldham, K. B. and Zoski, C. G. *J. Electroanal. Chem. 370* (1994) 1.
30. Savéant, J.-M. and Tessier, D. *Faraday Discuss. Chem. Soc. 74* (1982) 57.
31. Wayner, D. D. M. and Parker, V. D. *Acc. Chem. Res. 26* (1993) 287.
32. Lamy, E., Nadjo, L. and Savéant, J.-M. *J. Electroanal. Chem. 78* (1977) 403.
33. (a) Egger, K. W. and Cocks, A. T. *Helv. Chim. Acta 56* (1973) 1516; (b) NIST Standard Reference Database 25; NIST *Structures and Properties Database* and Estimation Program 1991, U.S. Department of Commerce, Gaithersburg, MD 20899, 1991.
34. Antonello, S. and Maran, F. *J. Am. Chem. Soc. In press.*
35. (a) Severin, M. G., Farnia, G., Vianello, E. and Arévalo, M. C. *J. Electroanal. Chem. 251* (1988) 369; (b) Andrieux, C. P., Robert, M., Saeva, F. D. and Savéant J.-M. *J. Am. Chem. Soc. 116* (1994) 7864; (c) Andrieux, C. P., Savéant J.-M. and Tardy, C. *J. Am. Chem. Soc. 119* (1997) 11546.
36. For example, see: Gupta, N. and Linschitz, H. *J. Am. Chem. Soc. 119* (1997) 6384.
37. (a) Galus, Z. *Fundamentals of Electrochemical Analysis*, 2nd ed., Ellis Horwood, New York 1994, p. 458; (b) Biernat, J. and Baranowska-Zralko, M. *Electrochim. Acta 17* (1972) 1867; (c) Baranowska-Zralko, M. and Biernat, J. *Electrochim. Acta 17* (1972) 1877.
38. For example, see: Gutmann, V. *The Donor–Acceptor Approach to Molecular Interactions*, Plenum Press, New York 1978.

Received January 19, 1999.